Analysis of Pore Structure of Longmaxi Shale Using the Mercury Intrusion Porosimetry Technique

Botao Lin[1*], Zheng Jiang[2], Yao Chen[1], Mian Chen[1], Yan Jin[1], Bing Hou[1]
[1]State Key Lab State Key Laboratory of Petroleum Resources and Prospecting, China University of Petroleum, Beijing, 102249, China.
[2]College of Engineering, Peking University, Beijing, 100871, China.
[*]Corresponding author: PhD, SPE, Associate Professor, email: linbotao@vip.163.com

This paper was prepared for presentation at the International Symposium of the Society of Core Analysts held in Avignon, France, 8-11 September, 2014

ABSTRACT

Understanding the pore structure of shale has gained prominence in the exploration of shale gas as a new important source of energy, since the relative permeability of either oil or water phase is largely dependent on it. The detailed characterization of pore structure is made possible with the advent of the mercury intrusion porosimetry (MIP) technique. The technique is based on the correlation of intrusion pressure of non-wetting fluid (mercury) with pore size, and therefore produces quantitative representation of pore structure in terms of pore size distribution. In this study, shale cores sampled in situ were prepared at different granular sizes and hydration states. Supplementary structural experimental tests such as SEM and CT are also conducted in order to reveal the internal surface structure of the cores in a relatively qualitative manner. Finally, technical issues of the application of MIP on shale samples are discussed, and the structural results derived from the three techniques are evaluated with respect to shale performance in recovery activities.

INTRODUCTION

The pore structure predominantly controls the mechanic, seepage and storage properties of shale especially in the case of shale gas or oil reservoirs. The pore connectivity and network that determine the fluid flow and chemical transport are largely dependent on pore size distribution, which in turn is substantially affected by the clay content and organic matter (Hu et al. 2012, Kuila and Prasad 2013). The estimated ultimate recovery (EUR) of tight-gas reservoirs is also highly dependent on the characteristics of pore structure (Sakhaee-Pour and Bryant 2012). One of the most popular laboratory approaches to obtain a quantitative representation of the volume and density distribution of micropores (pores less than 2 nm diameter) and mesopores (pores with 2-50 nm diameter), the types of pores typical in shale reservoirs, is through mercury intrusion porosimetry (Kuila and Prasad 2013). The technique is based on the correlation of the applied pressure of non-wetting fluid (mercury) and the radius of the interconnected empty pores that are intruded by the fluid. In this study, cores were sampled from the outcrop of Longmaxi shale gas reservoir in Sichuan basin, China and

investigated for their pore feature and its implications on the storage and transport properties of the reservoir. The sampling process is illustrated in Fig.1.

Fig.1. Sampling process of Longmaxi shale for MIP tests

EXPERIMENTS AND DISCUSSION

The total organic content (TOC) of the Longmaxi shale was found to be 2.5~3.5 % (Wang et al. 2009). The mineralogical composition was analyzed through X-ray diffraction (XRD) analysis on the sample powder. The associated diffraction pattern given in Fig.2 shows that the major minerals of the sample include illite, kaolinite, quartz, carbonate, dolomite, goethite, pyrite and gibbsite. In addition, extracted clay portion of the sample was investigated for clay mineralogy following U.S. Geological Survey (USGS) laboratory manual methods for X-ray powder diffraction (USGS, 2001), disclosing that clay contributes 15.7% mass of the entire sample, comprising 94% illite, 3% kaolinite and 3% chlorite.

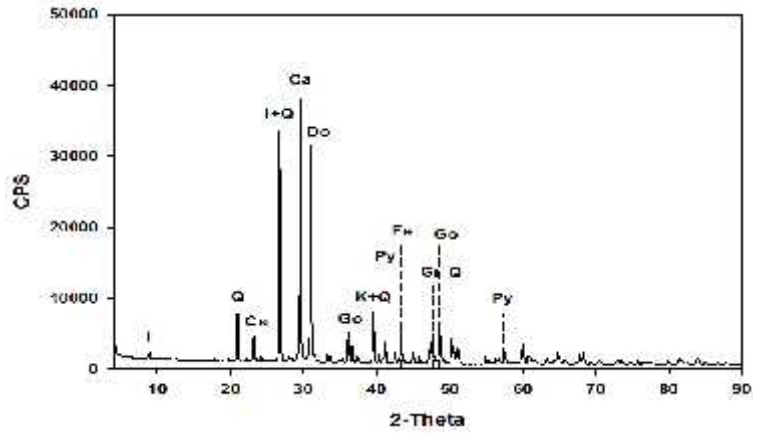

Fig.2. X-ray diffraction pattern of Longmaxi shale sample. CPS-counts per second, K-kaolinite, I-illite, Q-quartz, Ca-carbonate, Do-dolomite, Go-goethite, Py-pyrite, Gi-gibbsite

On the basis of mineralogical studies, it can be deduced that the Longmaxi shale is unlikely to experience volumetric expansion upon hydration since no expansive component (e.g., montmorillonite or vermiculite) is discovered. Therefore, the pore structure is not expected to be affected by hydration. In reverse, volumetric shrinkage after hydration due to oven drying is able to reorganize the clay particle alignment and change the pore space (Lin and Cerato 2013).

The shale samples used for MIP investigation were prepared in different granular sizes with their geometry listed in Table 1 below. Sample A was ground to pass US No. 20 sieve and has an average diameter less than 1 mm. The other samples (B~D) were crushed to flake-like configuration as shown in Fig.1 in order to fit the sample container. In addition, a sample (C2) hydrated with de-ionized water and then oven-dried was explored for its pore structure, which is compared to that without initial hydration (C1).

Table 1. Samples under MIP tests

Sample ID	Particle size and hydration state	Particle dimension (mm)				Porosity (%)
		Length	Width	Thickness	Average diameter	
A	powder_nonhydrated	-	-	-	<1	4.2
B	fine_nonhydrated	5	2	0.2	1.6	1.6
C1	medium_nonhydrated	7.5	3.5	2.6	5.1	2.3
C2	medium_hydrated	7.5	3.5	2.6	5.1	3.1
D	coarse_nonhydrated	10	5	5	7.8	2.2

The pore size distribution (PSD) can be represented by PSD density, or differential pore volume f(r), which is derived by (Li and Zhang 2009):

$$f(r)=\frac{dv(r)}{dr} \quad (1)$$

Where r and v(r) are pore radius and volume of pores with radii larger than r in 1 gram of dry rock. The relation curves of differential pore volume f(r) and the cumulative volume v(r) vs. pore radius r curves are provided in Fig.3 and Fig.4, respectively.

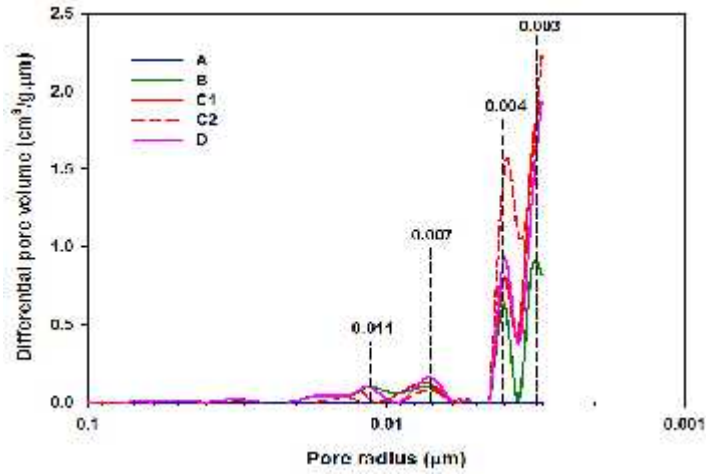

Fig.3. Differential pore volume vs. pore radius of the tested samples

For samples B, C1 and D, the accumulation of pore radii at 3 nm, 4 nm, 7 nm and 11 nm (defined as mesopores according to Kuila and Prasad 2013) is distinctive in Fig.3, with the first two peaks much more substantial than the rest two. The abrupt increases of slope in these curves at radius of 4 nm (Fig.4) further verify the significance of 3~4 nm mesopores. It is also implied in Fig.4 that the larger mesopores (7 and 11 nm) dominate

the pore volume of each sample, even though they exist in smaller number. In addition, the samples demonstrate similar peaks with the height increasing with increasing granular size. This trend may be attributed to fewer destructed pores that have internal walls turn to exposed surfaces when the grains become larger. On the other hand, the granular size has negligible effect on the cumulative pore volume and porosity as shown in Fig.4 and Table 1. An interesting phenomenon lies in the behavior of sample A. Pulverization reduced its peaks to almost align with the zero coordinate line (Fig.3), however, the cumulative volume is displayed as most significant, so is porosity (Fig.4 and Table 1). Apparently, such a behavior cannot be explained by the exposure of destructed pore walls as mentioned above, and warrants further research. Fig.4 also indicates that macropores of radii greater than 74 μm form major contribution to the total pore volume, even though they exist in small density (in Fig.3 the corresponding f(r) values are trivial and not shown for pore radii greater than 0.1 μm).

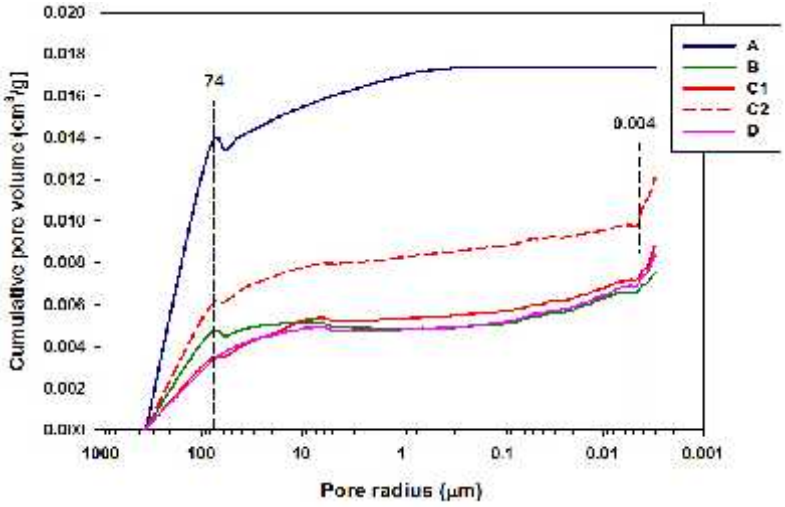

Fig.4. Cumulative pore volume vs. pore radius of the tested samples

The influence of hydration on the pore structure of shale is of critical importance in exploration of shale gas using hydraulic fracturing. To investigate this, sample C2 was hydrated for 48 hours in a chamber with vacuum applied to the chamber atmosphere. A close examination of the mineralogical makeup through XRD analysis discovered that no expansive mineral existed in the sample. Therefore, the pore shrinkage was explored through oven-drying of C2 after initial hydration. Fig.3 shows increased 3 and 4 nm peaks of C2 compared to those of C1, while its 7 and 11 nm peaks exhibit slight decreases. Meanwhile, the cumulative volume of C2 is about 1.5 times larger than that of C1 across the entire radius range (Fig.4), and its porosity is 35 % higher (Table 1). Considering these combined behaviors, it is proposed that shrinkage of clay and organic matter occurring after hydration generates new 3~4 nm mesopores while decreasing the number of 7~11 nm mesopores as a result of particle realignment, with the former effect outweighing the latter in changing cumulative volume.

The MIP approach has also been combined with the scanning electron microscopy (SEM) to understand the pore space characteristics or aid in improving the quality of

computer topography (CT) images in detecting structural and textural features in low porosity rocks, e.g., shale or carbonate (Fusi and Martinez-Martinez 2013). With this consideration, SEM and CT images of untreated Longmaxi shale core were achieved through laboratory tests and given in Fig.5.

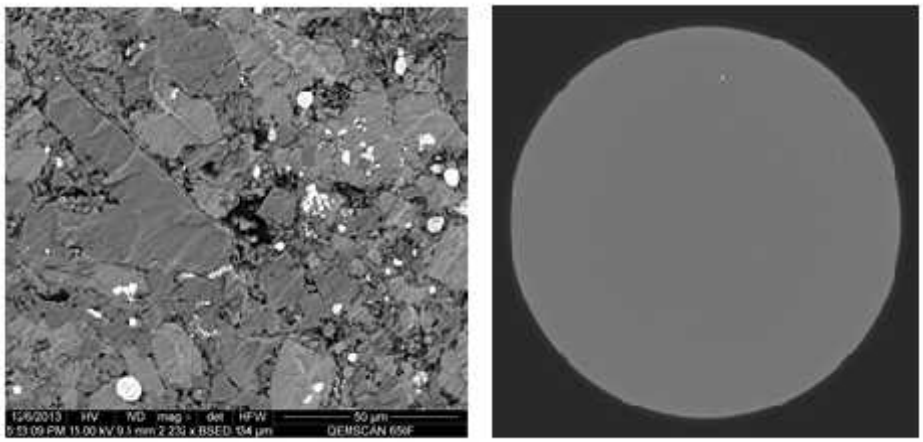

Fig.5. Microstructure of the shale sample—left: SEM image; right: CT image

Fig.5 illustrates the compact microstructure of Longmaxi shale with pore radius varying from less than 1 μm to approximately 12 μm. The SEM resolution of this study is unable to resolve geometric features of pores less than 1 μm. No specific structure feature is revealed by the CT image that covers a diameter of 25.4 mm with a voxel size of 13.3 μm besides indicating the compactness of the rock. SEM and CT imaging with higher resolution would be interesting, but was not taken at this stage for expenditure concerns.

CONCLUSION

In this study a series of laboratory tests were undertaken to aid in pore structure characterization of Longmaxi shale with emphasis focused on the MIP tests. Some conclusions can be drawn as follows.

The Longmaxi shale's pore structure is dominated by 3~11 nm mesopores or mesopore throats. The overall pore volume, on the other hand, is mostly determined by macropores larger than 74 μm though they occur in substantially lower frequencies. The SEM and CT approaches, on the other hand, are difficult to describe these characteristics provided the limited capacity of the apparatuses used.

The granular size has little impact on the differential and cumulative pore volume vs. pore radius result curves except for the pulverized one. The larger the sample grains, the more mesopores are conserved and therefore better representative of the actual pore structure. Samples with average diameter 2~8 mm are favorable for the MIP test purpose. Either too small (e.g., sample A in this case) or larger-size MIP samples are discouraged because the former exhibits abnormal behavior that is troublesome to interpret while the latter induces difficulty for mercury to intrude into the inner part of the grains. The use of pulverized sample should be especially avoided for MIP test purpose.

Shrinkage of clay and organic matter upon oven-drying on hydrated sample produces more 3~4 nm mesopores and slight decrease of the number of 7~11 nm. The cumulative pore volume, however, demonstrates overall increase over the pore radius range.

Additional research work is required to understand the pore structure evolution of shale through various scenarios it may experience in the exploration of shale gas and more rigorous physical simulation is desired. This research endeavor calls for other important techniques as well, such as isothermal gas adsorption, micro or nano-CT.

ACKNOWLEDGEMENTS

Financial support for this research was jointly provided the National Natural Science Foundation of China (Grants No. 51234006 and No. 51174217). The research work was also supported by Science Foundation of China University of Petroleum, Beijing (Grant No. 2462013YJRC037) and the Foundation of State Key Laboratory of Petroleum Resources and Prospecting (Grant No. PRP/indep-4-1309). These supports are greatly appreciated.

REFERENCES

Chen, W.L., Zhou, W., Luo, P., Deng, H.C., Li, Q., Shan, R. and Qi, M.H. (2013). Analysis of the shale gas reservoir in the lower Silurian Longmaxi formation, Changxin 1 well, southeast Sichuan basin, China. *Acta Petrologica Sinica*, 29 (3), 1073-1086.

Clarkson, C.R., Solano, N., Bustin, R.M., Bustin, A.M.M., Chalmers, G.R.L., He, L., Melnichenko, Y.B., Radlinski, A.P. and Blach, T.P. (2013). Pore structure characterization of North American shale gas reservoirs using USANS/SANS, gas adsorption, and mercury intrusion. *Fuel*, 103, 606-616.

Fusi, N. and Martinez, J.M. (2013). Mercury porosimetry as a tool for improving quality of micro-CT images in low porosity carbonate rocks. *Engineering Geology*, 166, 272-282.

Hu, Q., Ewing, R.P. and Dultz, S. (2012). Low pore connectivity in natural rock. *Journal of Contaminant Hydrology*, 133, 76-83.

Kuila, U. and Prasad, M. (2013). Specific surface area and pore-size distribution in clays and shales. *Geophysical Prospecting*, 61, 341-362.

Li, X. and Zhang, L.M. (2009). Characterization of dual-structure pore-size distribution of soil. *Canadian Geotechnical Journal*, 46, 129-141.

Lin, B. and Cerato, A.B. (2013). Hysteretic soil water characteristics and cyclic swell-shrink paths of compacted expansive soils. *Bulletin of Engineering Geology and the Environment*, 72 (1), 61-70.

Sakhaee-Pour, A. and Bryant, S.L. (2014). Effect of pore structure on the producibility of tight-gas sandstones. AAPG Bulletin, 98 (4), 663-694.

U.S. GEOLOGICAL SURVEY (2001). A Laboratory Manual for X-ray Powder Diffraction: USGS Open-File Report. http://pubs.usgs.gov/of/2001/of01-041/

Wang, S., Wang, L., Huang, J., Li, X. and Li, D. (2009). Accumulation conditions of shale gas reservoirs in Silurian of the Upper Yangtze region. *Natural Gas Industry*, 29(5), 45-50.